

# Microstructure modification of $\text{La}_2\text{Zr}_2\text{O}_7$ buffer films for coated conductors by metal organic decomposition

Jie Xiong · Xibin Wang · Pei Guo · Fei Zhang ·  
Yudong Xia · Cong Zhu · Pengju Xu ·  
Xiaohui Zhao · Bowan Tao

Received: 6 September 2012 / Accepted: 30 October 2012 / Published online: 7 November 2012  
© Springer Science+Business Media New York 2012

**Abstract**  $\text{La}_2\text{Zr}_2\text{O}_7$  (LZO) film directly deposited on Ni-5 at.%W by a chemical solution technique, metal organic decomposition (MOD), indicated a poor texture characteristic, which would result in high-angle grain boundaries in subsequent  $\text{YBa}_2\text{Cu}_3\text{O}_{7-\delta}$  (YBCO) associated with weak-link behavior. Different ultrathin MOD-LZO,  $\text{Y}_2\text{O}_3$ , and  $\text{CeO}_2$  seed layers ( $\sim$  several nanometers) with various annealing temperature were inserted to improve the crystallographic alignment. The relation between the texture and annealing temperature was systematically investigated. A  $\text{CeO}_2$  seed layer allows us to grow high quality LZO epitaxial films with values of full width at half-maximum around  $5.61^\circ$  and  $5.13^\circ$  for the  $\Phi$ -scan of (222) and rocking curve of (400) LZO, respectively, which is comparable to the microstructure of films grown using physical vapor deposited  $\text{Y}_2\text{O}_3$  as a seed layer. This buffer template, serving for YBCO coated conductors, could potentially decrease the overall fabrication cost.

## 1 Introduction

The development of the second-generation high-temperature superconductor (2G HTS) wires based on yttrium barium copper oxide (YBCO) is promising for electric power applications, such as power cables, transformers and

current limiters. [1–3] To fabricate YBCO films with high current carrying capability on metal substrates, two well established techniques to induce crystallographic alignment in YBCO films, i.e., rolling assisted biaxially textured substrate (RABiTS) [4] and ion-beam assisted deposition (IBAD) [5], have been mostly investigated. In the RABiTS approach, typical tri-layer stacks of  $\text{CeO}_2/\text{YSZ}/\text{Y}_2\text{O}_3$  are the most commonly explored architectures, [6, 7] i.e.,  $\text{Y}_2\text{O}_3$  film is used as a seed layer, YSZ (Y-stabilized Zirconia) plays a major role of diffusion barrier, while  $\text{CeO}_2$  cap layer provides better chemical compatibility and good lattice matching for the subsequent YBCO layer.

However, some challenges such as process complexity and high manufacturing cost are still present. It should be noted that a single buffer architecture has been developed recently, such as  $\text{Y}_2\text{O}_3$  [8],  $\text{CeO}_2$  [9],  $\text{LaMnO}_3$  [10], and  $\text{SrTiO}_3$  [11]. As a promising candidate of buffer material for YBCO coated conductors,  $\text{La}_2\text{Zr}_2\text{O}_7$  (LZO) material is currently of great interest because of its scalability, compatibility with YBCO material, the small lattice mismatch of the  $a$  or  $b$  axis with that of YBCO ( $\sim 0.5$  and  $1.8\%$ , respectively), the relatively low formation temperature of  $\sim 900^\circ\text{C}$ , the high stability of up to  $1,500^\circ\text{C}$  and the capability to grow biaxially textured on flexible textured substrate, acting both as a Ni diffusion barrier layer and as a seeding for the upper layers [12].

In the present work, we have employed a chemical solution deposition technique, metal-organic decomposition (MOD), to grow epitaxial LZO films on metal substrate. Chemical solution deposition for the growth of thin films provides advantages such as low cost, easy setup, and large area coating. Caroff et al. [13] reported a simple low cost architecture  $\text{YBCO}_{\text{MOCVD}}/\text{LZO}_{\text{MOD}}/\text{NiW}_{\text{RABiTS}}$ . Unfortunately, insufficient biaxial texturing of the LZO layer had been obtained and resulted in the problems

J. Xiong (✉) · X. Wang (✉) · P. Guo · F. Zhang · Y. Xia ·  
C. Zhu · P. Xu · X. Zhao · B. Tao  
State Key Laboratory of Electronic Thin Films and Integrated  
Devices, University of Electronic Science and Technology of  
China, Chengdu 610054, People's Republic of China  
e-mail: jixiong@uestc.edu.cn

X. Wang  
e-mail: wangxibin12@163.com

associated with weak-linked, high-angle grain boundaries. To improve microstructure and enhance electric properties, physical vapor deposited (PVD)- $\text{Y}_2\text{O}_3$  seed layers were inserted to improve the LZO buffer texture [14]. However, for the development of cost-effective all-solution approaches, MOD-seed layers are necessary to replace the PVD-seed layers with improved the texture of LZO films.

In this paper, we report our efforts to grow high quality LZO films on ultrathin seed layers such as LZO,  $\text{CeO}_2$  and  $\text{Y}_2\text{O}_3$  by all-MOD technique. We show the results of a systematic study of orientation variety of LZO films as a function of annealing temperature, and show the effect of the MOD-seed coatings on the texture of LZO layer.

## 2 Experimental

The biaxially textured Ni-5 at.%W (Ni-W) tape was supplied by EVICO GmbH with 10 mm in width and 80  $\mu\text{m}$  in thickness. Before spin-coating, the substrates were cleaned in an ultrasonic bath filled with acetone and ethanol for 5 min, respectively, and annealed at 700  $^\circ\text{C}$  for 15 min in a reducing atmosphere ( $\text{Ar}/5\% \text{H}_2$ ). Propionic acid ( $\text{CH}_3\text{CH}_2\text{COOH}$ ) was used as the solvent for all precursor solutions. The LZO precursor solution was prepared from Lanthanum(III) 2,4-pentanedionate ( $\text{La}[\text{CH}_3\text{COCHCOCH}_3]_3 \cdot x\text{H}_2\text{O}$ , Alfa Aesar) and Zirconium(IV) 2,4-pentanedionate ( $\text{Zr}[\text{CH}_3\text{COCHCOCH}_3]_4$ , Alfa Aesar). After adding the propionic acid, the precursor solution was placed into an oil bath pan with continuous stirring at 95  $^\circ\text{C}$  for 30 min in a reduced pressure distillation equipment. The total cation concentration was about 0.6 mol/l ( $\text{La}:\text{Zr} = 1:1$ ). For  $\text{Y}_2\text{O}_3$ ,  $\text{CeO}_2$  seed layers precursor solution, yttrium(III) acetate tetrahydrate ( $\text{Y}[\text{OOCCCH}_3]_3 \cdot 4\text{H}_2\text{O}$ , Alfa Aesar) and cerium(III) 2,4-pentanedionate hydrate ( $\text{Ce}[\text{C}_5\text{H}_7\text{O}_2]_3 \cdot x\text{H}_2\text{O}$ , Alfa Aesar) were adopted. The cation concentrations of the precursor solutions of LZO,  $\text{Y}_2\text{O}_3$ ,  $\text{CeO}_2$  seed layers were 0.04, 0.02, 0.02 mol/l, respectively. Seed layers were spin-coated at a spin rate of 3,200 rpm for 60 s in glove box and then crystallized at 700–900  $^\circ\text{C}$  for 30 min in a flowing mixture of  $\text{Ar}/5\% \text{H}_2$  gas. Following LZO buffer films were deposited on the crystallized seed layers at 1,800 rpm for 40 s and heat-treated at 1,100  $^\circ\text{C}$  for 1 h. The rapid heating and cooling process was utilized, and significantly shorten the preparation time and helped to obtain high-quality textured LZO films.

X-ray diffraction ( $\theta - 2\theta$ ,  $\omega$ -scan and  $\Phi$ -scan) was used to characterize the phase purity and textures of LZO buffer films using Bede D1 X-ray diffractometer with  $\text{Cu K}\alpha$  radiation. The surface morphology was investigated using atomic force microscope (AFM, Seiko SPA300HA microscope).

## 3 Results and discussion

### 3.1 LZO/Ni-W

LZO films were directly deposited on Ni-W substrates by spin-coating and annealed at different temperature from 900 to 1,100  $^\circ\text{C}$ . The thickness of a single-coated LZO films was about 64 nm, obtained by X-ray Reflectivity (XRR), shown in Fig. 1. The epitaxial nature of LZO films was investigated using XRD  $\theta - 2\theta$  scan, shown in Fig. 2. There are only ( $h00$ ) reflections of LZO except for the peaks from the substrates, indicating that all the films were good epitaxial with  $a$ -axis perpendicular to the substrate. No grains with other orientation and no impurity phases were detected in the films.

With the increase of annealing temperature from 900 to 1,100  $^\circ\text{C}$ , the intensity of LZO (400) reflections varied

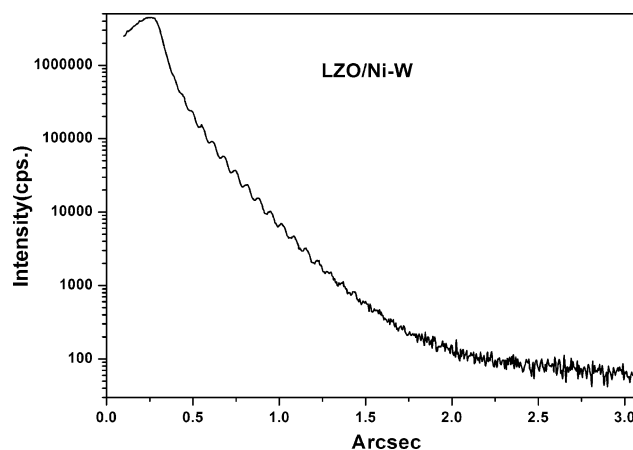


Fig. 1 Typical XRR curve of LZO film on Ni-W substrate

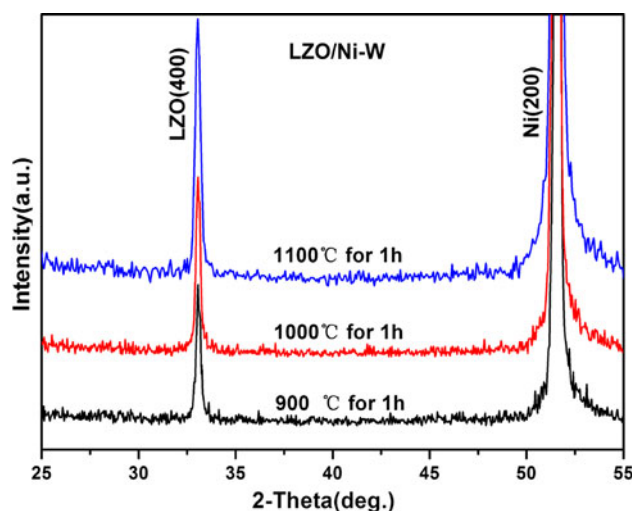
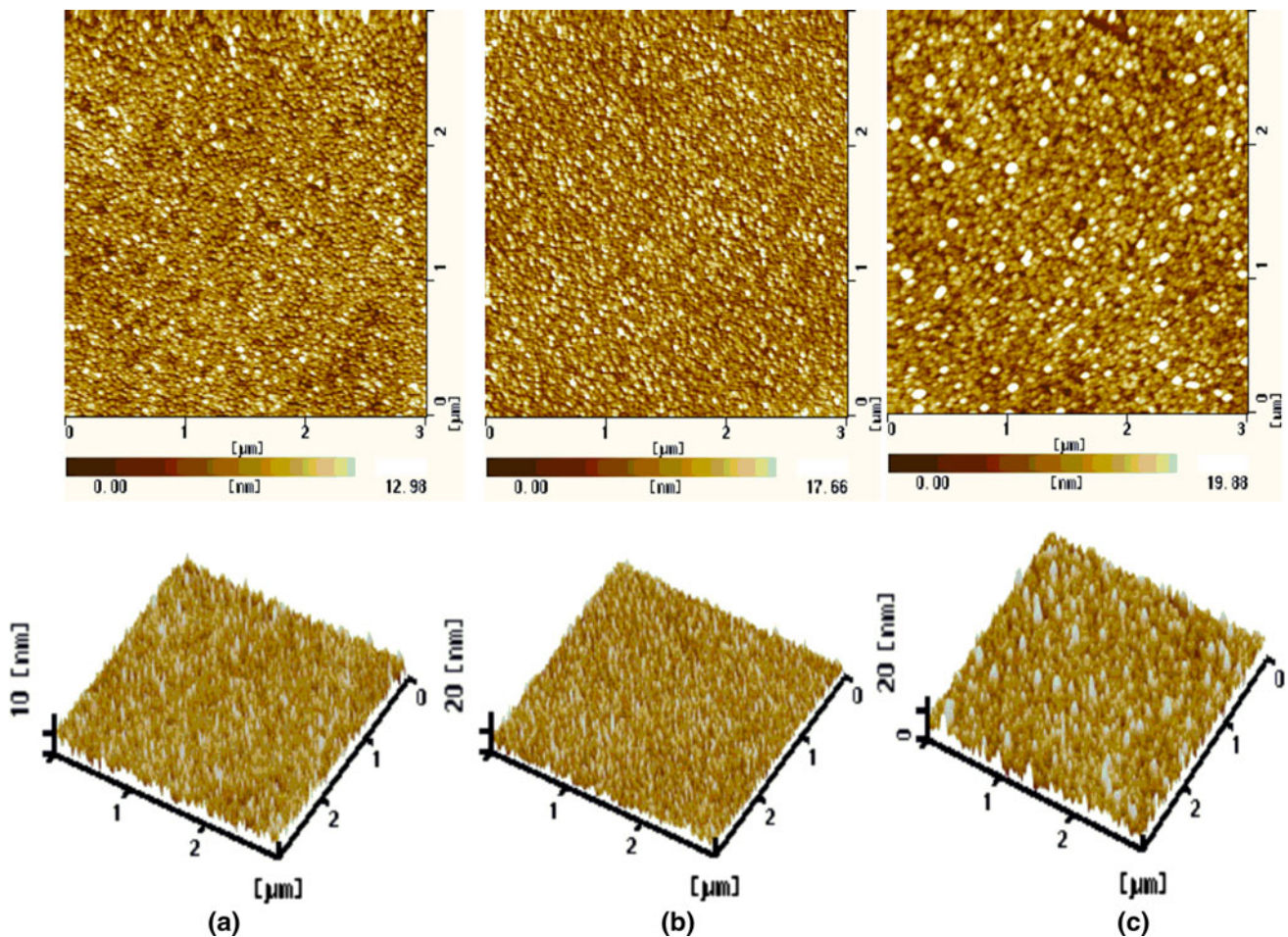


Fig. 2 XRD  $\theta - 2\theta$  patterns of LZO films directly grown on Ni-W substrates annealed at different temperature



**Fig. 3** AFM 2D and 3D images showing the surface morphologies of **a** MOD-LZO seed layer annealing at 900 °C, **b** MOD-Y<sub>2</sub>O<sub>3</sub> seed layer annealing at 800 °C, **c** MOD-CeO<sub>2</sub> seed layer annealing at 800 °C. The rms roughness are 2.03, 2.69, 3.12 nm, respectively

from 620 to 1,180 cps (counts per second), demonstrating that LZO films had better crystallinity at a higher annealing temperature ( $T_A$ ). The out-of-plane mosaics ( $\Delta\omega$ ) of LZO annealed at different temperature were 7.19°, 6.92°, 6.92° and the in-plane texture ( $\Delta\Phi$ ) were 6.20°, 6.16°, 6.20°, respectively, shown in Fig. 4a, indicating no degrading in the out-of-plane texture and a deteriorative in-plane texture compared to the underlying substrate.

Though it is a respectable microstructure comparable to other groups [14–16], it is still far from the performance of the all-PVD buffer stack, typical out-of-plane crystallographic texture of 3.4°, and in-plane of 5.1° [17]. Therefore, further optimization of the solution buffer stack is required.

### 3.2 MOD-seed/Ni-W

Before LZO coating, ultrathin LZO, Y<sub>2</sub>O<sub>3</sub> and CeO<sub>2</sub> films, serving as the seed layers, were spin-coated on Ni-W substrates, respectively. From XRD  $\theta - 2\theta$  patterns which were not shown here, no any diffraction peaks from the

seed layer were observed, attributing to too thin films (~several nanometers). AFM investigations of the surface morphology of different seed layers annealed at 800–900 °C indicated a compact, crack free surface structure with an average grain size of about 50 nm, as shown in Fig. 3. Over the 3  $\mu\text{m} \times 3 \mu\text{m}$  scan area, the root mean square (rms) surface roughness of the MOD-seed layers were 2.03 nm (LZO-seed), 2.69 nm (Y<sub>2</sub>O<sub>3</sub>-seed) and 3.12 nm (CeO<sub>2</sub>-seed), respectively, representing a very smooth surface, which were beneficial for subsequent LZO buffer layer epitaxial growth.

### 3.3 MOD-LZO/MOD-seed/Ni-W

To evaluate the effect of texture, 64 nm-thick LZO films under the same coating conditions were deposited on different MOD-seed layers with various annealing temperature from 700 to 1,100 °C. Figure 4b–d shows the relation between the LZO crystallographic texture and the annealing temperature of MOD-seed layers. For MOD-LZO itself as seed layer, the out-of-plane texture of LZO buffer films

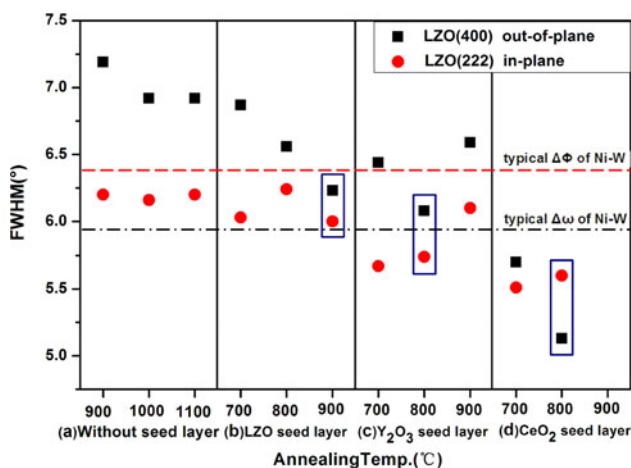


**Fig. 4** The crystallographic texture of LZO buffer films grown on different seed layers which annealed at different temperature **a** without seed layer, **b** MOD-LZO seed layer, **c** MOD-Y<sub>2</sub>O<sub>3</sub> seed layer, **d** MOD-CeO<sub>2</sub> seed layer

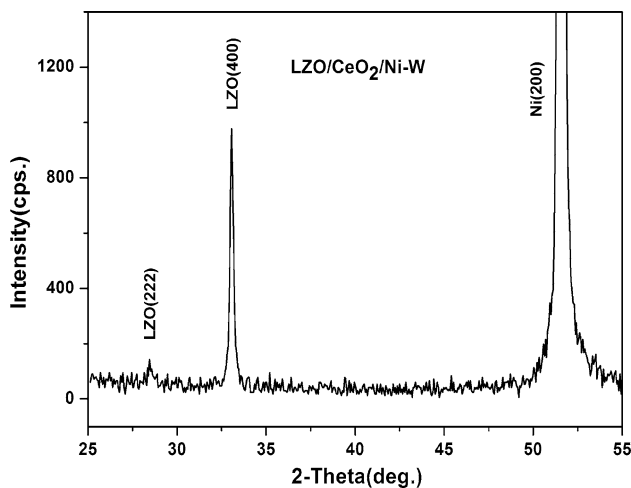


**Fig. 5** XRD  $\theta - 2\theta$  pattern of LZO/MOD-CeO<sub>2</sub>/Ni-W film. CeO<sub>2</sub> seed layers was annealed at 800 °C

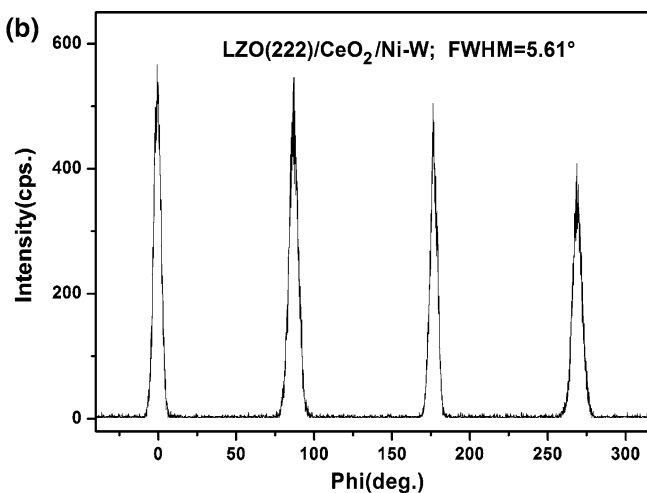
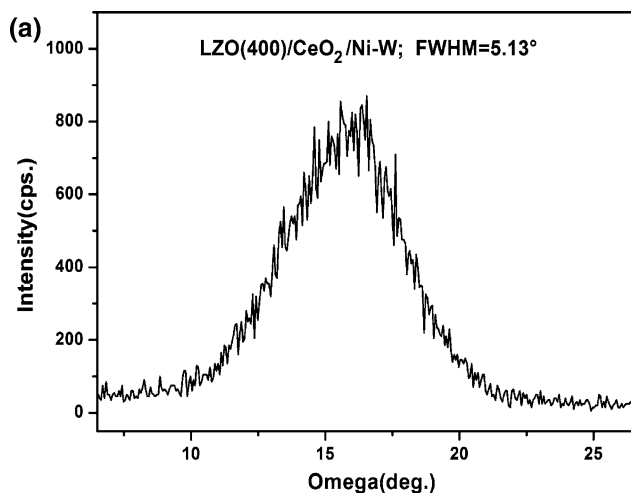


**Fig. 6** **a** XRD rocking curve and **b**  $\Phi$ -scan of LZO/MOD-CeO<sub>2</sub>/Ni-W film

improved 0.7° when the LZO seed layer annealed at 900 °C, whereas there are not any improvement in the in-plane texture comparable to the LZO without seed layer (in Fig. 4a, b). For MOD-Y<sub>2</sub>O<sub>3</sub> seed layer,  $\Delta\omega$  and  $\Delta\Phi$  of LZO buffer films are 6.08° and 5.74° ( $T_A = 800$  °C), indicating slightly improvement in comparison with MOD-LZO seed (Fig. 4c).

The typical XRD  $\theta - 2\theta$  pattern of a LZO films grown on a seed CeO<sub>2</sub> buffered Ni-W substrate is shown in Fig. 5. It should be pointed out that there is a weak peak at  $2\theta = 28.5^\circ$ , can be attributed to LZO (222). By comparing the relative intensities of the bragg peaks associated with the LZO (400) and LZO (222), we estimate that  $\sim 96$  % of the LZO is *a*-axis oriented.

The out-of-plane and in-plane crystallographic alignments of LZO/CeO<sub>2</sub>/Ni-W film were investigated by XRD rocking curve and  $\Phi$ -scan, shown in Fig. 6. Four peaks with a separation of 90° in the LZO (222)  $\Phi$ -scan indicate the epitaxial nature of the films. The out-of-plane mosaic ( $\Delta\omega$ ) of LZO is 5.13° and the in-plane texture ( $\Delta\Phi$ ) is 5.61°, indicating a significant improvement in the in-plane and out-of-plane textures. These values are comparable with those of LZO films on physical vapor deposited seed layer [13]. The mechanism of the in-plane and out-of-plane texture improvement of LZO films on CeO<sub>2</sub> seed layer is not fully understood yet. We, however, believe that the much finer grain size may make the texture evolution easier and helps the growth of high quality LZO films. The texture improvement can be also attributed to the grain growth competition at high temperature, similar to the commonly observed phenomena in thin film microstructural evolution [18].

These results demonstrate the feasibility of using a seed CeO<sub>2</sub> buffered LZO template, and as such a major advance in the field to fabricate CCs with reduced number of

processing steps and potentially reduced manufacturing costs. It should be noted that more work is needed to further optimize the process and to fabricate high performance YBCO superconducting layer, which we believe should be possible.

#### 4 Conclusion

We had demonstrated that epitaxial LZO films were obtained on textured Ni-W substrates by MOD method with and without the seed layers. A significant improvement in the in-plane and out-of-plane textures in the LZO layers was observed by inserting different MOD-LZO,  $Y_2O_3$ , and  $CeO_2$  between LZO films and the substrate. A combination of ultrathin seed  $CeO_2$  and buffer LZO layers revealed the best values, i.e.,  $5.61^\circ$  and  $5.13^\circ$  for in-plane texture and out-of-plane mosaic, respectively. This offers the promise to the development of an all-solution approach with performance comparable to the all-PVD buffer stack, and thus a potentially lower-cost alternative for conductor fabrication.

**Acknowledgments** We gratefully acknowledge the support of 863 High-Tech Project (No. 2009AA03Z201) and the National Science Foundation of China under Grant No. 50902017 for this work.

#### References

1. R.A. Badcock, N.J. Long, M. Mulholland et al., *IEEE Trans. Appl. Supercond.* **19**, 3244 (2009)
2. N. Glasson, M. Staines, R. Buckley et al., *IEEE Trans. Appl. Supercond.* **21**, 1393 (2011)
3. W. Schmidt, B. Gamble, H.P. Kraemer et al., *Supercond. Sci. Technol.* **23**, 1 (2010)
4. A. Goyal, M. Paranthaman, U. Schoop, *Mater. Res. Soc.* **29**, 552 (2004)
5. N.A. Paul, R.F. Stephen, *Mater. Res. Soc.* **29**, 543 (2004)
6. J. Xiong, Y. Chen, Y. Qiu et al., *J. Mater. Sci. Technol.* **23**, 457 (2007)
7. X. Li, M.W. Rupich, T. Kodenkandath et al., *IEEE Trans. Appl. Supercond.* **17**, 3553 (2007)
8. D.Q. Shi, R.K. Ko, K.J. Song et al., *Supercond. Sci. Technol.* **18**, 561 (2005)
9. J. Xiong, Y. Chen, Y. Qiu et al., *Supercond. Sci. Technol.* **19**, 1068 (2006)
10. T. Aytug, M. Paranthaman, S. Kang et al., *IEEE Trans. Appl. Supercond.* **13**, 2661 (2003)
11. J.T. Dawley, R.J. Ong, P.G. Clem, *J. Mater. Res.* **17**, 1678 (2002)
12. L. Molina, H. Tan, E. Biermans et al., *Supercond. Sci. Technol.* **24**, 065019 (2011)
13. T. Caroff, S. Morlens, A. Abrutis et al., *Supercond. Sci. Technol.* **21**, 075007 (2008)
14. S. Sathyamurthy, M. Paranthaman, L. Heatherly et al., *J. Mater. Res.* **21**, 910 (2006)
15. K. Knoth, B. Schlobach, R. Huhne et al., *Phys. C* **426**, 979 (2005)
16. T. Caroff, S. Morlens, A. Abrutis et al., *Supercond. Sci. Technol.* **21**, 075007 (2008)
17. Y.D. Xia, J. Xiong, F. Zhang et al., *Phys. C* **476**, 48 (2012)
18. J. Xiong, V. Matias, H. Wang et al., *J. Appl. Phys.* **108**, 083903 (2010)